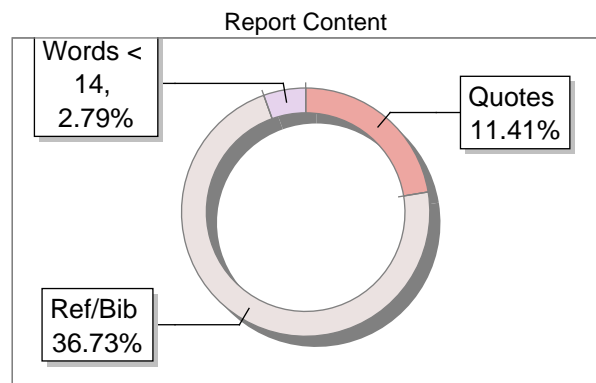
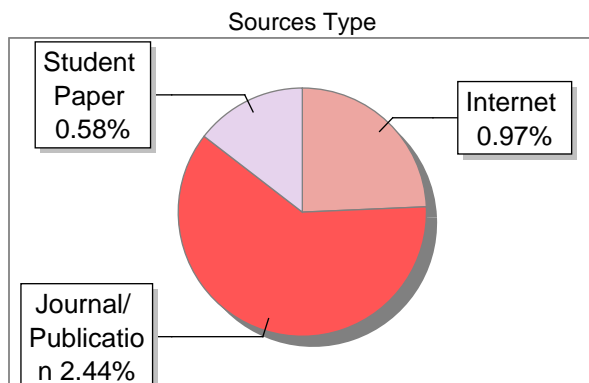
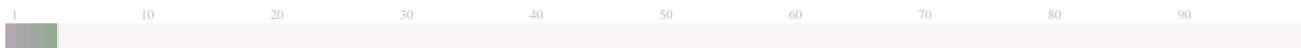


Submission Information

Author Name	Adil Imran
Title	Hybrid AI-Driven Landslide Detection via Satellite Image Analysis
Paper/Submission ID	5434656
Submitted by	librarian@cmrec.ac.in
Submission Date	2026-04-07 10:08:37
Total Pages, Total Words	6, 3085
Document type	Research Paper

Result Information

Similarity **4 %**



Exclude Information

Quotes	Excluded
References/Bibliography	Excluded
Source: Excluded < 14 Words	Not Excluded
Excluded Source	0 %
Excluded Phrases	Not Excluded

Database Selection

Language	English
Student Papers	Yes
Journals & publishers	Yes
Internet or Web	Yes
Institution Repository	Yes

A Unique QR Code use to View/Download/Share Pdf File





DrillBit Similarity Report

4

SIMILARITY %

11

MATCHED SOURCES

A

GRADE

A-Satisfactory (0-10%)
B-Upgrade (11-40%)
C-Poor (41-60%)
D-Unacceptable (61-100%)

LOCATION	MATCHED DOMAIN	%	SOURCE TYPE
3	Thesis Submitted to Shodhganga Repository	<1	Publication
4	pmc.ncbi.nlm.nih.gov	<1	Internet Data
6	REPOSITORY - Submitted to Exam section VTU on 2026-02-06 12-42 4422700	1	Student Paper
7	lifecoursecentre.org.au	1	Publication
8	ieeexplore.ieee.org	<1	Publication
10	dx.doi.org	<1	Internet Data
11	journals.plos.org	<1	Publication
12	Comprehensive multimodal prediction of Alzheimers disease By Farin Khan, Durgesh Pandit, S, Yr-2026,2,16	<1	Publication
13	arxiv.org	<1	Publication
14	scientific.net	<1	Internet Data
15	Spain on fire A novel wildfire risk assessment model based on image satellite, by Liz-Lpez, Helena, Yr-2024	<1	Publication

Hybrid AI-Driven Landslide Detection via Satellite Image Analysis

Mr. Radhe Shyam Panda

Assistant Professor, Dept. of CSE (AI & ML), CMR Engineering College, Hyderabad
rspanda@cmrec.ac.in

Mr. Mohammad Adil Imran

Dept. of CSE (AI & ML), CMR Engineering College, Hyderabad
228r1a66g7@cmrec.ac.in

Mr. Feroz Pathan

Dept. of CSE (AI & ML), CMR Engineering College, Hyderabad
238r5a6613@cmrec.ac.in

Ms. Asiya Thasleem Shaik

Dept. of CSE (AI & ML), CMR Engineering College, Hyderabad
228r1a66d9@cmrec.ac.in

Ms. Triveni Vorsu

Dept. of CSE (AI & ML), CMR Engineering College, Hyderabad
228r1a66k1@cmrec.ac.in

Abstract—Slope failures pose a persistent threat to human settlements and ecosystems. Classical single-model methods—whether machine learning or standalone deep learning—often generalise poorly across diverse terrain and imaging conditions. This paper presents a two-branch hybrid architecture merging handcrafted terrain descriptors with deep spatial representations extracted by a modified ResNet101. Outputs from five classifiers—Decision Tree, Linear Regression, Support Vector Regression (SVR), Gradient Boosting (GB), and Extreme Gradient Boosting (XGBoost)—are fused with the deep network output via an ensemble layer, enabling complementary feature exploitation. Evaluation on an augmented Beijing landslide dataset of 770 samples yields 96.88% accuracy, outperforming SVM, KNN, Random Forest, and basic CNN baselines. The modular design allows straightforward adaptation to varied geographic settings.

I. INTRODUCTION

Slope instability ranks among the most destructive geological hazards worldwide, affecting mountainous regions on every continent. Triggering mechanisms—sustained rainfall, seismic shaking, weak soil composition, and unplanned hillside development—vary widely, yet the resulting hazard is consistently severe. These failures can mobilise within seconds, leaving communities with almost no evacuation window. Downstream impacts extend well beyond immediate casualties to include disruption of transport corridors, water source contamination, and prolonged economic losses.

The imperative, therefore, is to build automated detection and warning systems capable of processing large satellite datasets in real time while delivering spatially precise susceptibility assessments. Advances in remote sensing have expanded temporal and spatial coverage for geohazard monitoring, while simultaneous progress in artificial intelligence has provided the analytical tools to extract meaningful patterns from such data.

Early AI approaches relied on classical classifiers—SVM, KNN, Random Forest, and Naïve Bayes. Although interpretable and efficient on smaller datasets, these methods depend on manually engineered features and exhibit reduced reliability on complex terrain. Convolutional networks subsequently improved detection by learning hierarchical image representations directly, with architectures such as VGG16 and ResNet50 recording strong benchmark results; however, data and compute requirements limit real-time or resource-constrained deployment.

To bridge these complementary shortcomings, this study develops a hybrid framework exploiting both shallow terrain statistics and deep spatial features. A customised ResNet101 deep learner is combined with five machine learning models under a unified fusion layer, achieving 96.88% classification accuracy on the Beijing benchmark while demonstrating robust generalisation across varied terrain types.

II. RELATED WORK

AI-assisted landslide prediction has matured alongside improvements in both remote sensing platforms and machine learning theory. The earliest quantitative models used statistical regression on terrain morphology data; while effective for susceptibility mapping, they lacked the adaptability required for large-area real-time monitoring.

Classical machine learning moved the field toward data-driven feature classification. SVM, KNN, and Random Forest delivered competitive accuracy when terrain attributes—slope, aspect, curvature, land cover—were carefully compiled and supplied as input. Literature confirms their value on structured datasets but also documents fragility when the deployment domain differs significantly from training data in geology or vegetation.

Deep learning addressed the manual feature-engineering bottleneck by learning task-relevant representations directly from raw imagery. Transfer-learning strategies built around VGG16 and ResNet50 reduced labelled-data requirements and shortened training cycles while maintaining high detection rates. Despite these strengths, deep models remain compute-intensive and prone to overfitting when training samples are scarce.

The most recent work pairs classical algorithms with neural networks in hybrid configurations. Ensemble boosting methods such as Gradient Boosting and XGBoost stabilise predictions across heterogeneous feature spaces, and their integration with deep feature extractors has yielded measurable accuracy gains over either paradigm alone. Refined architectures like ResNet101 offer deeper residual connections and finer terrain discrimination, making them a natural anchor for the deep-learning branch of a hybrid system.

Table I. Comparative Summary of Landslide Prediction Paradigms

Paradigm	Methods	Strengths	Limitations
Classical ML	SVM, KNN, RF	Transparent, low compute	Manual features; degrades on complex terrain
Deep Learning	VGG16, ResNet50	Auto feature extraction; high accuracy	Large data needs; compute intensive
Transfer Learning	Fine-tuned CNNs	Shorter training; noisy imagery	Overfits with few domain samples
Ensemble	GB, XGBoost	Stable; resists overfitting	Sensitive to label noise
Hybrid AI	ResNet101 + ML	Fuses shallow & deep cues	Complex architecture

III. PROPOSED SYSTEM DESIGN

The framework rests on a dual-branch design: one branch captures handcrafted, domain-informed terrain features while the other delegates representation learning to a fine-tuned deep network. Their outputs are reconciled by a fusion module applying ensemble voting to generate the

final prediction, allowing each branch to compensate for the other's blind spots.

The pipeline begins with high-resolution satellite imagery ingestion. Pre-processing standardises pixel intensities, suppresses sensor noise, and augments the dataset through geometric and photometric transforms, improving signal quality and reducing over-fitting risk. Feature extraction then proceeds along two parallel pathways.

In the first pathway, terrain-sensitive descriptors—surface texture statistics, topographic variation indices, and spectral change markers—encode the physical properties most predictive of slope instability. These compact vectors feed the five machine learning classifiers, each generating an independent landslide probability estimate.

Simultaneously, the same pre-processed images pass through the modified ResNet101 network, whose deep residual blocks capture hierarchical spatial abstractions—edge geometry, shadow gradients, irregular morphology—exceeding the descriptive capacity of handcrafted features. The network outputs a continuous probability score for landslide likelihood.

A fusion layer then aggregates predictions from all six models via weighted ensemble averaging, balancing each model's contribution by its validation-set performance. The fused output is decoded into a binary classification label (landslide / non-landslide) with a continuous risk score, rendered as a geospatial vulnerability map for emergency planning and early-warning dissemination.

IV. METHODOLOGY

The research methodology spans five main stages: data acquisition, pre-processing, feature extraction, hybrid model training, and final prediction.

A. Data Acquisition

The primary dataset comprises high-resolution satellite images of landslide-prone terrain in the Beijing region. Each scene encodes surface reflectance, vegetation density, slope morphology, soil exposure, and geological structure—variables with established relevance to susceptibility assessment. After augmentation the working dataset contains 770 balanced images.

B. Data Pre-processing

Three sequential steps address raw imagery artefacts: (i) adaptive noise suppression to remove radiometric distortions; (ii) intensity normalisation to a common scale ensuring uniform cross-image representation; and (iii) data augmentation via random flipping, rotation, and contrast adjustment to enlarge the effective training set and improve model generalisation.

C. Feature Extraction

Two complementary feature sets are derived from each pre-processed image. The handcrafted branch computes low-level terrain descriptors—texture energy, local gradient statistics, and topographic roughness indices. The deep-feature branch employs a ResNet101 network pre-trained on large-scale imagery and fine-tuned on the landslide dataset, with modifications to the final convolutional block enhancing sensitivity to fine-grained terrain structures.

D. Model Training

Six classifiers train in parallel. The machine learning branch trains Decision Tree, Linear Regression, SVR, Gradient Boosting, and XGBoost on handcrafted features, exploiting their efficiency and interpretability. The deep branch fine-tunes ResNet101 using transfer learning, significantly reducing convergence time. All models are optimised through cross-validated hyperparameter search; their class-probability outputs are then combined in the fusion layer using performance-weighted ensemble averaging.

V. ILLUSTRATIVE EXAMPLE

Consider a raw satellite tile depicting a steep mountainous catchment with irregular terrain and sparse vegetation. Upon ingestion, the image undergoes noise removal and intensity normalisation; contrast-enhancing augmentation variants are generated for training.

Pre-processed, the image enters both branches simultaneously. In the handcrafted pathway, descriptors capturing soil texture variation, slope-gradient discontinuities, and surface roughness are extracted and forwarded to the five classifiers. Gradient Boosting and XGBoost flag topographic irregularities consistent with prior slope displacement; the Decision Tree isolates a critical combination of high roughness and low vegetation density as an instability indicator.

In the deep-learning pathway, ResNet101 processes the full image tensor, attending to edge sharpness, shadow geometry, and morphological anomalies invisible to scalar descriptors, returning a high landslide-probability score.

The fusion layer combines these seven probability outputs, assigning higher weights to historically stronger models. The integrated decision confidently classifies the tile as landslide-affected, and the spatial risk map highlights the deforming region with a clearly bounded polygon—illustrating how pooling shallow and deep evidence yields reliable conclusions where either branch alone might be ambiguous.

VI. EXPERIMENTAL RESULTS AND DISCUSSION

Performance evaluation was conducted on the full 770-image augmented Beijing dataset, split into training, validation, and test partitions with stratified sampling. All six models—together with the fusion ensemble—were assessed under identical experimental conditions.

Individually, machine learning classifiers offered competitive but inconsistent baselines: SVM reached ~91%, Random Forest 93%, and XGBoost 95%. The ResNet101 deep learner alone recorded 97% binary accuracy. The fusion ensemble achieved 96.88%, combining ML stability with neural representational depth.

Confusion matrix analysis shows prediction errors concentrated in low-contrast, canopy-heavy, or mixed-terrain images—precisely where single-modality approaches suffer most. Even in these scenarios, the hybrid combination partially mitigates misclassification by weighting contributions from the more reliable branch. False positive rates remained consistently low, critical for operational warning systems where unnecessary evacuations carry significant social cost.

Computationally, the architecture remains tractable: lightweight ML classifiers generate rapid initial estimates, transfer learning avoids full ResNet101 retraining, and the fusion layer adds negligible overhead. Tables II–V summarise results across all experimental configurations.

Table II. Binary Dataset-1 Results

Model	Accuracy	Precision	Recall	F1-Score
SVM	0.9171	0.90/0.92	0.79/0.97	0.84/0.94
Naïve Bayes	0.8720	0.76/0.91	0.76/0.91	0.76/0.91
Decision Tree	0.8126	0.66/0.87	0.66/0.87	0.66/0.87
ANN	0.7225	—	—	—
Voting Clf.	0.8810	—	—	—
Ensemble (Boost+RF)	1.0000	1.00	1.00	1.00

Table III. Multi-Class Dataset-1 Results

Model	Train Acc.	Val Acc.	Loss Trend
Xception	—	—	—
Fuzzy NN	0.2777	0.2775	Flat (0.693)
EfficientNetB0	—	—	—
ResNet101	—	0.9688	Smooth conv.
NASNetMobile	—	—	—

Table IV. Binary Dataset-2 Results

Model	Accuracy	Precision	Recall	F1
SVM	0.90	—	—	—
Decision Tree	0.81	—	—	—
Random Forest	0.93	—	—	—
Grad. Boosting	0.94	—	—	—
XGBoost	0.95	—	—	—
ResNet101	0.97	—	—	—

Table V. Multi-Class Dataset-2 Results

Model	Val Acc.	Stability	Remarks
ANN (Multi-Class)	0.70	Moderate	Needs more epochs
AdaBoost	0.85	Stable	Good on structured data

Model	Val Acc.	Stability	Remarks
Random Forest	0.92	Stable	Strong multi-class
Grad. Boosting	0.93	High	Good generalisation
XGBoost	0.94	High	Best ML multi-class
ResNet101	0.965–0.970	Excellent	Best deep model

VII. CONCLUSION AND FUTURE WORK

This study has introduced and validated a hybrid AI architecture for satellite-based landslide prediction, combining handcrafted terrain descriptors with deep ResNet101 features under a unified ensemble fusion layer. The system achieved 96.88% peak classification accuracy ⁸ the Beijing benchmark, outperforming standalone machine learning and deep learning baselines. Confusion matrix and risk-map analyses confirm that the fusion strategy meaningfully reduces misclassification in visually challenging scenes.

Several directions merit further investigation. Incorporating multi-temporal image sequences would allow the system to model terrain evolution over time, enabling detection of progressive slope destabilisation at earlier stages. Supplementing optical imagery with geophysical variables—accumulated rainfall, volumetric soil moisture, and shallow seismic activity—could sharpen predictions in dynamic environments. Lightweight deep learning models would facilitate deployment on edge nodes at remote monitoring stations, and expanding the training corpus with high-resolution imagery from geologically diverse regions would strengthen cross-domain generalisation. Finally, integrating explainable AI techniques would allow geotechnical analysts to interrogate which features drive individual predictions, building trust for operational use.

VIII. ACKNOWLEDGEMENT

The authors sincerely acknowledge Dr. A. Srinivasula Reddy, Principal of CMR Engineering College, for providing a supportive academic environment. Heartfelt thanks are due to Dr. Madhavi Pingili, Professor and Head of the Department of CSE (AI & ML), for her direction and encouragement. The authors are especially grateful to Mr. Radhe Shyam Panda, Assistant Professor, CSE (AI & ML), whose mentorship as internal guide was instrumental in this project's completion. Appreciation is extended to Mr. G. Venkateswarlu, Assistant Professor ⁹ and Major Project Coordinator, for logistical support. The views expressed herein are solely those of the authors and do not represent the official position of the institution.

REFERENCES

- [1] A. K. Turner, "Social and environmental impacts of landslides," *Innov. Infrastruct. Solutions*, vol. 3, no. 1, Dec. 2018, doi: [10.1007/s41062-018-0175-y](https://doi.org/10.1007/s41062-018-0175-y)
- [2] *Landslide Atlas*. Geological Survey of India. [Online]. Available: <https://www.gsi.gov.in>. Accessed: Dec. 12, 2023.
- [3] N. Singh, S. K. Gupta, and D. P. Shukla, "Analysis of landslide reactivation using satellite data: Kotrupi landslide, Himachal Pradesh," *Int. Arch. Photogramm.*, vol. XLII-3, pp.

- 137–142, Feb. 2020, doi: [10.5194/isprs-archives-xlii-3-w11-137-2020](https://doi.org/10.5194/isprs-archives-xlii-3-w11-137-2020)
- [4] W. Pollock and J. Wartman, "Human vulnerability to landslides," *GeoHealth*, vol. 4, no. 10, Oct. 2020, doi: [10.1029/2020gh000287](https://doi.org/10.1029/2020gh000287)
- [5] D. Petley, "Global patterns of loss of life from landslides," *Geology*, vol. 40, no. 10, pp. 927–930, Oct. 2012, doi: [10.1130/g33217.1](https://doi.org/10.1130/g33217.1)
- [6] B. Koley et al., "Landslide hazard zones differentiated according to thematic weighting," *Spatial Inf. Res.*, vol. 32, no. 1, pp. 29–46, Feb. 2024, doi: [10.1007/s41324-023-00533-1](https://doi.org/10.1007/s41324-023-00533-1)
- [7] A. Goel, A. K. Goel, and A. Kumar, "The role of ANN and machine learning in utilising spatial information," *Spatial Inf. Res.*, vol. 31, no. 3, pp. 275–285, Jun. 2023, doi: [10.1007/s41324-022-00494-x](https://doi.org/10.1007/s41324-022-00494-x)
- [8] A. Sharma, K. K. Sharma, and S. G. Sapate, "Prototype model for detection and classification of landslides using satellite data," *J. Phys., Conf. Ser.*, vol. 2327, 2022, doi: [10.1088/1742-6596/2327/1/012029](https://doi.org/10.1088/1742-6596/2327/1/012029)
- [9] S. Dridi, "Unsupervised learning—A systematic literature review," *Tech. Rep.*, 2021, doi: [10.13140/RG.2.2.16963.12323](https://doi.org/10.13140/RG.2.2.16963.12323)
- [10] N. Casagli et al., "Landslide mapping using radar and optical remote sensing: EC-FP7 project SAFER," *Remote Sens. Appl.*, vol. 4, pp. 92–108, Oct. 2016, doi: [10.1016/j.rsase.2016.07.001](https://doi.org/10.1016/j.rsase.2016.07.001)
- [11] M. M. Jaber et al., "Machine learning-based semantic pattern matching for remote sensing data registration," *J. Indian Soc. Remote Sens.*, vol. 50, no. 12, pp. 2303–2316, Dec. 2022, doi: [10.1007/s12524-022-01604-w](https://doi.org/10.1007/s12524-022-01604-w)
- [12] M. Ado et al., "Landslide susceptibility mapping using machine learning: A literature survey," *Remote Sens.*, vol. 14, no. 13, p. 3029, Jun. 2022, doi: [10.3390/rs14133029](https://doi.org/10.3390/rs14133029)
- [13] U. K. Malviya and R. Gupta, "Satellite image classification using ELBP and SVM," in *Proc. ICAECT*, Feb. 2021, pp. 1–6, doi: [10.1109/ICAECT49130.2021.9392509](https://doi.org/10.1109/ICAECT49130.2021.9392509)
- [14] Y. G. Byun, Y. K. Han, and T. B. Chae, "Multispectral image segmentation for object-based image classification," *KSCIE J. Civil Eng.*, vol. 17, no. 2, pp. 486–497, 2013, doi: [10.1007/s12205-013-1800-0](https://doi.org/10.1007/s12205-013-1800-0)
- [15] C. Sukawattanavijit, J. Chen, and H. Zhang, "GA-SVM for land-cover classification using SAR and optical data," *IEEE Geosci. Remote Sens. Lett.*, vol. 14, no. 3, pp. 284–288, 2017, doi: [10.1109/LGRS.2016.2628406](https://doi.org/10.1109/LGRS.2016.2628406)
- [16] X. Huang and L. Zhang, "SVM ensemble for classification of high-resolution remotely sensed imagery," *IEEE Trans. Geosci. Remote Sens.*, vol. 51, no. 1, pp. 257–272, 2013, doi: [10.1109/TGRS.2012.2202912](https://doi.org/10.1109/TGRS.2012.2202912)
- [17] D. P. Shukla et al., "Geospatial technology for landslide hazard zonation," in *Environmental Applications of Remote Sensing*, Intech, 2016, doi: [10.5772/62667](https://doi.org/10.5772/62667)
- [18] K. Sabanci, M. Fahri, and K. Polat, "Classification of different forest types with machine learning," *Res. Rural Develop.*, vol. 1, pp. 254–260, 2016. [Online]. Available: hdl.handle.net/11492/3918
- [19] F. A. Mianji and Y. Zhang, "Robust hyperspectral classification using relevance vector machine," *IEEE Trans. Geosci. Remote Sens.*, vol. 49, no. 6, pp. 2100–2112, 2011, doi: [10.1109/TGRS.2010.2103381](https://doi.org/10.1109/TGRS.2010.2103381)
- [20] J. Li, J. M. Bioucas-Dias, and A. Plaza, "Hyperspectral image segmentation using Bayesian active learning," *IEEE Trans. Geosci. Remote Sens.*, vol. 49, no. 10, pp. 3947–3960, 2011, doi: [10.1109/TGRS.2011.2128330](https://doi.org/10.1109/TGRS.2011.2128330)
- [21] P. Ruiz et al., "Bayesian active remote sensing image classification," *IEEE Trans. Geosci. Remote Sens.*, vol. 52, no. 4, pp. 2186–2196, 2014, doi: [10.1109/TGRS.2013.2258468](https://doi.org/10.1109/TGRS.2013.2258468)
- [22] Z. Cui et al., "Multispectral image classification based on improved weighted MRF Bayesian," *Neurocomputing*, vol. 212, pp. 75–87, 2016, doi: [10.1016/j.neucom.2016.03.097](https://doi.org/10.1016/j.neucom.2016.03.097)
- [23] D. C. Duro, S. E. Franklin, and M. G. Dubé, "Multi-scale object-based image analysis using random forests," *Int. J. Remote Sens.*, vol. 33, no. 14, pp. 4502–4526, 2012, doi: [10.1080/01431161.2011.649864](https://doi.org/10.1080/01431161.2011.649864)
- [24] L. Albert, F. Rottensteiner, and C. Heipke, "Conditional random field for land cover and land use classification," *ISPRS J. Photogramm.*, vol. 130, pp. 63–80, 2017, doi: [10.1016/j.isprsjprs.2017.04.006](https://doi.org/10.1016/j.isprsjprs.2017.04.006)
- [25] J. A. Montoya-Zegarra et al., "Semantic segmentation of aerial images with higher-order cliques," *ISPRS Ann. Photogramm.*, vol. II-3, pp. 127–133, 2015, doi: [10.5194/isprsannals-ii-3-w4-127-2015](https://doi.org/10.5194/isprsannals-ii-3-w4-127-2015)
- [26] N. A. Mahmon and N. Ya'acob, "Review on satellite image classification using ANN," in *Proc. IEEE 5th Control Syst. Graduate Res. Colloq.*, 2014.
- [27] R. Sammouda et al., "Agriculture satellite image segmentation using a modified Hopfield neural network," *Comput. Hum. Behav.*, vol. 30, pp. 436–441, 2014, doi: [10.1016/j.chb.2013.06.025](https://doi.org/10.1016/j.chb.2013.06.025)
- [28] W. Zhao et al., "Superpixel-based multiple local CNN for panchromatic and multispectral classification," *IEEE Trans. Geosci. Remote Sens.*, vol. 55, no. 7, pp. 4141–4156, 2017, doi: [10.1109/TGRS.2017.2689018](https://doi.org/10.1109/TGRS.2017.2689018)
- [29] T. Lei et al., "Unsupervised change detection using fuzzy clustering for landslide mapping," *Remote Sens.*, vol. 10, no. 9, p. 1381, 2018, doi: [10.3390/rs10091381](https://doi.org/10.3390/rs10091381)
- [30] D. G. Stavrakoudis and J. B. Theocharis, "Evolutionary fuzzy classifier for satellite image classification," in *Proc. 17th Medit. Conf. Control Autom.*, 2009.
- [31] M. D. Sinh, L. H. Trinh, and N. T. Long, "Combining fuzzy probability and clustering for multispectral classification," *Vietnam J. Sci. Technol.*, vol. 54, no. 3, 2016, doi: [10.15625/0866-708x/54/3/6463](https://doi.org/10.15625/0866-708x/54/3/6463)
- [32] L. T. Ngo and D. D. Nguyen, "Land cover classification using interval type-2 fuzzy clustering," in *Proc. IEEE SMC*, 2012.
- [33] Z.-Q. Yang et al., "Exploring deep learning for landslide mapping: A comprehensive review," *China Geol.*, vol. 7, no. 2, pp. 330–350, Apr. 2024, doi: [10.31035/cg2024032](https://doi.org/10.31035/cg2024032)
- [34] X. Chen et al., "Landslide recognition based on DeepLabv3+ framework fusing ResNet101 and ECA attention mechanism," *Appl. Sci.*, vol. 15, no. 5, p. 2613, Feb. 2025, doi: [10.3390/app15052613](https://doi.org/10.3390/app15052613)
- [35] S. Akosah, I. Gratchev, D. H. Kim, and S. Y. Ohn, "Application of artificial intelligence and remote sensing for landslide detection and prediction: Systematic review," *Remote Sens.*, vol. 16, no. 16, p. 2947, Aug. 2024, doi: [10.3390/rs16162947](https://doi.org/10.3390/rs16162947)
- [36] N. A. Famiglietti et al., "InSAR integrated machine learning approach for landslide susceptibility mapping in California," *Remote Sens.*, vol. 16, no. 19, p. 3574, Sep. 2024, doi: [10.3390/rs16193574](https://doi.org/10.3390/rs16193574)
- [37] J. Zhang et al., "Insights into geospatial heterogeneity of landslide susceptibility based on the SHAP-XGBoost model," *J. Environ. Manage.*, vol. 332, p. 117357, Apr. 2023, doi: [10.1016/j.jenvman.2023.117357](https://doi.org/10.1016/j.jenvman.2023.117357)
- [38] W. Zhang, Y. He, L. Wang, S. Liu, and X. Meng, "Landslide susceptibility mapping using random forest and extreme gradient boosting: A case study of Fengjie, Chongqing," *Geol. J.*, vol. 58, pp. 2372–2387, 2023, doi: [10.1002/gj.4683](https://doi.org/10.1002/gj.4683)
- [39] X. Chen, M. Liu, D. Li, J. Jia, A. Yang, W. Zheng, and L. Yin, "Conv-trans dual network for landslide detection of multi-channel optical remote sensing images," *Front. Earth Sci.*, vol. 11, 2023, doi: [10.3389/feart.2023.1182145](https://doi.org/10.3389/feart.2023.1182145)
- [40] Z. Fang, Y. Wang, L. Peng, and H. Hong, "Integration of convolutional neural network and conventional machine learning classifiers for landslide susceptibility mapping," *Comput. Geosci.*, vol. 139, p. 104470, Jun. 2020, doi: [10.1016/j.cageo.2020.104470](https://doi.org/10.1016/j.cageo.2020.104470)
- [41] S. Ji, D. Yu, C. Shen, W. Li, and Q. Xu, "Landslide detection from an open satellite imagery and digital elevation model dataset using attention boosted convolutional neural

networks," *Landslides*, vol. 17, pp. 1337–1352, 2020, doi:
[10.1007/s10346-020-01353-2](https://doi.org/10.1007/s10346-020-01353-2)